European Space Agency detector development for space science: present and future activities

Duvet L. [a], Bavdaz M. [a], Crouzet P.E. [a], Nelms N.[b], Nowicki-Bringuier Y. R.[b], Shortt B. [a], Verhoeve P. [a]

[a] Future mission preparation office, Directorate of Science and Robotic Exploration, ESA/ESTEC, Keplerlaan 1, 2200AG Noordwijk, The Netherlands;
[b] Opto-electronics section, Directorate of Technical Quality and Management, ESA/ESTEC, Keplerlaan 1, 2200AG Noordwijk, The Netherlands

ABSTRACT

We report on the present and future detector development activities for the European Space Agency Science Programme. The development of European technology in that field is a key mission enabler for the program, which requires TRL6 (ISO scale) by end of the definition phase, so called "mission adoption". This is particularly true for Astronomy and fundamental physics type missions. Current activities are in particular targeting large format and p-channel CCD, NIR and MWIR, LWIR wavelength ranges as well as related ASIC controller. For the longer term future mission plan (so called M4, M5 and L2 missions, M3 being PLATO and L1 JUICE), the extreme ends of the spectrum will be addressed. An overview of the detector status for the Earth Observation program is given in appendix, as most of the technologies are directly applicable to some extent to science missions, in particular for Planetary missions. The specific validation activities in place in the future mission preparation office in support to the space science program will be eventually briefly detailed.

Keywords: Detector, CCD, NIR, TES, CIS, MWIR, LWIR, ESA

1. INTRODUCTION

This paper provides a status of the present and future activities for the detector developments at the European Space agency for the science program, so called Cosmic Vision.
The first section provides an overview of the Cosmic Vision program and status as well as a brief description of the associated Technology Development process managed by ESA to respond to the need of the missions in the program.
The second section will review in details the status of the different detector technologies addressed by the current and future technology development activities of the science program with decreasing wavelength range, starting with Long Wave Infrared (LWIR), ending with gamma ray detectors.
The last section will provide an insight on the dedicated on-going and foreseen internal validation activities put in place by the Science and Robotic Exploration directorate at ESTEC.
In appendix, the status of the developments driven by the Earth Observation Program and potentially interesting for space science, are given to provide a complete picture.

2. ESA SCIENTIFIC PROGRAM AND TECHNOLOGY DEVELOPMENT PROCESS

2.1 ESA scientific mission program

All ESA member states participate (on a Gross National Product basis) in activities related to space science and a common set of programmes (so called Mandatory programmes). The associated general budget comprises future studies, technological research, education. For Science, Solar system, astronomy and fundamental physics

Further author information: (Send correspondence to L. Duvet, N. Nelms)
L. Duvet E-mail: ludovic.duvet@esa.int, Telephone: +31715656209
N. Nelms E-mail: nick.nelms@esa.int, Telephone: +31715658110

High Energy, Optical, and Infrared Detectors for Astronomy VI, edited by Andrew D. Holland, James Beletic, Proc. of SPIE Vol. 9154, 915403 · © 2014 SPIE · CCC code: 0277-786X/14/$18 · doi: 10.1117/12.2069310

are part of the mandatory programmes. In addition, member states choose their level of participation in optional programmes (Human spaceflight, Telecommunications and integrated Applications, Earth Observations, launchers, navigation, Space Situational Awareness and Robotic Exploration). The overall science programme is managed by the Directorate of Science and Robotic Exploration.
The building blocks of the science program plan are:

- L and M missions in implementation and planned (Bepi Colombo, Solar Orbiter, Euclid, JUICE...)
- L and M missions in operation (XMM, Integral, Mars Express, Cluster, Rosetta...)
- Small missions (to be confirmed as long-term elements of the Science Programme pending successful implementation of the S1 mission CHEOPS[1])
- Mission of opportunity, which are small contributions to missions led by partner agencies (Microscope, Hinode, PROBA-2)
- Basic activities: preparation for the future, technology and science management support activities.

All ESA science missions are selected via open calls to the science community. The current science program is built around the "Cosmic Vision" which plans to address 4 fundamental questions:

- What are the conditions for the conditions for planetary formation and the emergence of life?
- How does the Solar system work?
- What are the physical fundamental laws of the Universe?
- How did the Universe originate and what is it made of?

The missions are classified in 4 groups:

- L-missions: large european flagship with a cost to ESA of around 2 annual budget year, one very 7-8 years. L1 is JUICE[2] (2022), L2 is an X-ray observatory (to be launched in 2028) and L3 will address gravity waves (to be launched in 2034)
- M-missions: ESA led or implemented with international collaboration. The cost to ESA is around one annual budget, one every 3-4 years. M1 is Solar orbiter[3] (launch in 2017), M2 is Euclid[4](launch in 2020), M3 is PLATO[5] (PLAnetary Transits and Oscillations of Star), recently selected after competition with ECHO (Exoplanet Characterization Observatory), LOFT (The large Observatory for X-ray Timing), MARCO-POLO R and STE-QUEST (Space-Time Explorer and QUantum Equivalence Principle Space Test). M4 call will be in 2014 for a launch in 2026 and M5 call in 2015 for a launch in 2030.
- S-missions: cost capped missions allowing national agencies to play a larger role, 0.1 annual budget, one every 4-5 years. S1 is CHEOPS.
- O-missions: mission of "Opportunity", led by other agencies, small contributions (so far SPICA[6])

The mission cycle at ESA can be divided in 3 main phases in terms of management and responsibilities:

- Future mission preparation addressing all activities from mission call until mission adoption at the end of phase B1
- Project implementation managing all activities related to implementation, from phase B2 until in-flight commissioning
- Operation taking over after the in flight commissioning until end of mission.

The success of these missions relies greatly on a successful and complete technology development plan initiated during the complete phase of future mission preparation.

2.2 Cosmic Vision Technology Development plan

The Cosmic Vision Technology Development plan (TDP) defines the technology development activities that are needed for enabling the implementation of the Cosmic Vision missions with a satisfactory Technology Readiness Level (TRL), with a targeted TRL $\geq 6^*$ by mission adoption.
Mainly two ESA budgets are used to achieve this goal:

- Technology Research Programme (TRP), addressing low TRLs (TRL 3-4)

*This level is achieved for a technology when the associated critical functions are verified, the performances are demonstrated in the relevant environment and model(s) in form, fit and function is(are) available[7] by mission adoption. For detectors on board space missions, radiations is typically one of the key environment issue.

- Science Core Technology Programme (CTP) for reaching TRL6 and beyond

The available time for technology preparation is:

- 3-4 years for M missions
- 6-7 years for L missions

The TDP comprises two groups of activities. The first related to the spacecraft elements, is developed by ESA, and is funded and implemented by the ESA Science Programme. The second, related to the payload elements that are planned to be provided by the Member States, is to be funded and implemented by the member States and is referred to as "National Activities". It is worth mentioning that for some astronomy missions for which payload elements like detectors are seen as a high risk, ESA can take the lead. This was the case for GAIA and Euclid and will be the case for PLATO for which large CCD focal plane arrays are under National agencies responsibility while the CCD pre-development, development and procurement are under ESA authority.
The technology activities are always on the critical path of the schedule for all missions and a close coordination with the Member states is necessary for maintaining the Cosmic Vision schedule.
Nearly all activities are mission specific, a few CTP activities (∼10-15 %) are however multi-mission long-term activities, following a careful selection and prioritization done by the ESA science Advisory structure. The TDP is regularly[8](typically one per year) to take into account the program's evolutions. We will address in this paper only the detector technology development activities funded and managed by ESA in the current TDP. Synergy with other ESA programs like the Earth Observation Program (EOP) is insured by the Technology Directorate at ESTEC (European Space Technical Center).

3. STATUS OF THE DETECTOR DEVELOPMENT ACTIVITIES FOR THE SPACE SCIENCE PROGRAM

This section provides a status of the present and planned detector technology activities for the ESA future science missions, essentially for Astronomy. For each activity, the goals as well as latest results (whenever possible) are given. As a last point, long-term technologies, not yet in the program but considered, will be addressed.

3.1 Bolometers for far infrared and (sub)-millimeter applications

Detectors based on the registration of a temperature rise induced by the absorption of photon energy hold the promise of extremely high sensitivity when operated at very low temperature. They usually consist of an absorber with heat capacity C, a temperature sensor (e.g. a temperature dependent resistor) and a weak link with thermal conductance G to the thermal bath. Their sensitivity scales as $NEP \approx \sqrt{4gkT^2G}$ (Noise Equivalent Power)for bolometers, and $\Delta E \approx \sqrt{kT^2C}$ for photon counting microcalorimeters. Here g=0.5-1.0, T is the detector temperature. The typical response time constant for these devices is =C/G. Transition Edge Sensors (TES) operated in Electro-Thermal Feedback mode (ETF)[9] are excellent candidates as thermometers for these devices. They consist of a superconducting material which is voltage biased in its superconducting transition at T=Tc. The steepness of this transition makes them both very sensitive, and, through the ETF mechanism, enhances their speed of response significantly. In addition, they can be made in large monolithic arrays through micromachining and lithographic fabrication techniques. Being low impedance devices, they can be conveniently readout in multiplexed mode by using Superconducting Quantum Interference Devices (SQUIDs) as amplifiers and switches.
Major performance improvements of future FIR (Far InfradRed) and sub-millimeter missions beyond the successful Herschell observatory lie primarily in enhanced sensitivity. This requires a colder telescope in order to suppress the background to below the sky background, as well a more sensitive detectors so as to be sky background limited. A European FIR Imaging Fourier spectrometer instrument SAFARI[10] onboard the Japanese SPICA mission[11] has been proposed and studied as an M3 mission candidate until February 2014. Typical requirements for the detectors on such an instrument include: $NEP \sim 2\ 10^{-19}$ W/$\sqrt{Hz}$, saturation power ∼10 fW, detector speed ∼100Hz, pixel sizes 0.5-1.5 mm, array formats 500-2000 pixels, wavelength band 34-210 μm, operational temperature (Tc) 100mK. ESA is pursuing the development of TES-based bolometers for such applications, as well as the development of a SQUID based multiplexed readout system. An initial development activity led by Cardiff University has resulted in well-defined fabrication procedures for arrays of TES (at Cambridge University, UK, and SRON, the Netherlands), see Figure 1, as well as a concept for micromachined horn

arrays for optical coupling (RAL, UK) and a set of tools for end-to-end simulation of the optical performance (Maynooth University, Ireland). Performance close to the above mentioned requirements (including dark NEP$\sim$4 10^{-19} W/$\sqrt{Hz}$) was already demonstrated[12,13]. A follow-on activity (Cardiff University, Cambridge University) is ongoing, with the aim to improve the NEP of single pixels and arrays and identify physical limits of the TES technology , to improve the optical performance as well as the optical characterization of these sensitive detectors, and to increase the TRL of the technology through developments in the area of system design, manufacturing, assembly and packaging (large arrays). A separate activity for development of SQUIDs and Frequency Domain Multiplexed (FDM) readout of AC-biased TES bolometers (led By SRON (the Netherlands), with VTT (Finland), PTB (Germany),Thales-Alenia Space (Italy)), has demonstrated the feasibility of multiplexing large numbers of TESs at sufficiently low noise level[14]. This development will largely be applicable to the readout of x-ray TESs (see section 3.5).

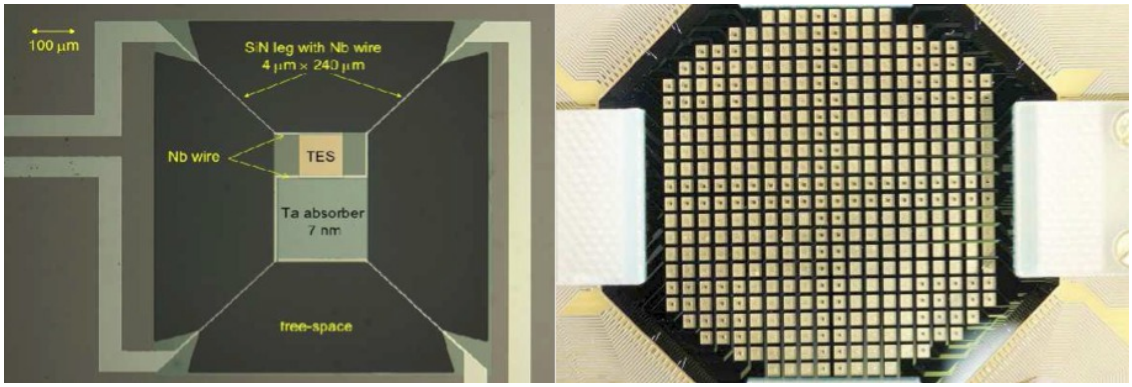

Figure 1: left single pixel TiAu TES (SRON, the Netherlands) right: array of 488 TESs for the wavelength band 110-210 μm (Cambridge University, UK)

3.2 MWIR to LWIR

MCT detectors are up to now the reference choice for detectors covering SWIR to VLWIR range : the possibility to tune the bandgap of this ternary alloy to adjust the detection range, the rather important availability of stable manufacturers and designs and the relative maturity of this material used for a few decades in military applications makes it attractive also for space applications.
One of the driver requirement conditioning future scientific missions (as well as earth observation missions) is the dark Current figure achievable. Indeed, future missions, planned at mid or long term, require levels of dark currents several orders of magnitude lower than what is currently obtained among available technologies. The objective of dark current reduction is twofold : on one hand, to increase the detection performances by limiting this parasitic contribution, on the other hand, at given optical performances, to enable an increase of the operational temperature of the detector. The potential overall system impact at spacecraft level is very large. A relevant illustration of this need is the former M3 mission candidate EChO.[15] The baseline design incorporated 5 spectrometer bands from VNIR (visible up to 2.5 μm) to LWIR (11 μm to 16 μm) as shown on figure 2. For MWIR channels Teledyne detectors used on NEOCAM[16] were baselined with target dark currents of 100 e/s at operating temperature, a QE $\geq$ 50% as major drivers. Due to the need of a large dynamic range to accommodate both bright targets and faint targets, the concept of the instrument required at detector level :

- High Dynamic range with in particular very low ROIC noise operation, in particular for bright targets.
- Very low dark current for each band.
- Consequently low temperature operation plus strong limitation on the possibility to warm up the detectors, due to power constraints.

These requirements were identified as very challenging, in particular for an instrument covering such a wide detection range. Consequently, several programs were initiated in Europe with different strategies:

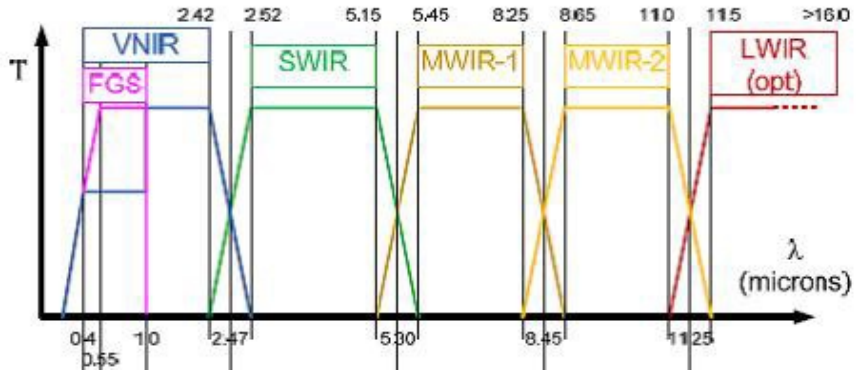

Figure 2: Echo channels[17]: Fine Guidance Sensor/Visible (channel 1), VNIR (channel 2), SWIR (channel 3), MWIR-1 (channel 4), MWIR-2 (channel 5) and LWIR (channel 6) optional.

- Possibility to cool down existing off-the-shelf European detectors to reach the dark current target.
- Improving the current MCT technologies further to reduce the dark current to a lower level, for a given temperature. The activity Low Dark Current 2D MCT VLWIR detectors, although focused primarily on Earth Observation VLWIR needs, has a common target with the scientific goal of EChO-like missions in that respect. Refer to section A.1 for more details.
- A third activity, which is planned to be launched end 2014, aims at going further in implementing both readout integrated circuit and improved detection layers compatible with low temperature low dark current operation.

3.2.1 Cryogenic testing of existing detectors

For this activity, two parallel contracts, one with CEA (France, LETI for manufacturing IRFU for testing) and another one with AIM (Germany) have been initiated and recently completed. Using off-the-shelf ROIC (Readout Circuitry), limitations were obviously expected. The targeted wavelengths range were specifically channel 3, 4 and 5 as defined on figure 2.
The Detectors manufactured by the CEA/LETI were made on LPE standard n/p for channel 3 and 4, p/n for channel 5 using standard technology production available at SOFRADIR. In total 7 devices have been tested: 2 devices for channel 3 (typically λc=6.5 μm at 78K) and 5 (typically λc=11.9 μm at 40K), 3 devices for channel 4 (typically λc=10.1 μm at 40K). The pixel size is 30 μm with a CTIA input stage, 320 x 340 matrix (referred as CL95), typical readout noise 700 e- at 80K. The main results are gathered in table 1. For channel 4, the

Channel	Quantum efficiency(%)	Temperature at which the dark current spec. is met (K)
Channel 3	$\geq$70% between 20K and 78 K	70 K
Channel 4	From 60% at 78 K to 30% at 20 K	Req. not met
Channel 5	From 85% at 78 K to 45% at 20 K	19 K

Table 1: Main results of the MWIR/LWIR detector tests for ECHO at CEA/LETI/IRFU. The dark current requirements of 100 e-/s for a 18 μm pixel scales to 278 e-/s for the 30 μm pixel.

dark current performances were not met but the cut-off was well the required one, there is confidence that the requirement could be eventually achieved. These QE measurements for channel 4 and 5 show that a contraction of the diffusion length with temperature lead to a decrease of the spectral response with decreasing temperature, the effect is accentuate for thicker detection layer, i.e. for increasing cut-off.
For AIM, 2 detectors on 24 μm pitch with CTIA architecture, 384x288 pixels were used per channel. The results

are however not yet available for publications.
Overall, these 2 activities have shown the potentials and limitations of the existing technology with very promising results for dark current. The correct behavior of the ROIC below 50 K obviously determines to a large extent the capability to characterize accurately the MCT performances.

3.2.2 Development of Low Dark Current 2D MWIR/LWIR detector

In order to overcome the limitations mentioned in section 3.2.1, a specific development is required. The activity Development of Low Dark Current 2D MWIR/LWIR detector activity aims at developing such a detector, with still EChO-like mission requirements. The main characteristics of this activity will be:

- From a material point of view, search for a detection layer able to sustain low temperature operation (i.e. down to values as reported in section 3.2.1), with very low dark current while maintaining good electro-optical performances (in particular Quantum Efficiency).
- From a ROIC point of view, development of a ROIC able to sustain low temperature operation with high dynamic range and in particular very low read-out noise operation.

At the time of writing of this paper, the call for this activity is in the process of being published for open competition, for a start expected end of the year 2014. Two parallel contracts will be awarded to pursue this development.

3.3 NIR

The ESA led activities for science in the NIR (up to 2.5 μm) are focused on Astronomy like missions requiring low noise, very low dark current and good QE. A specific development plan was defined in 2008 aiming at the capability to have a full detection system ("photon to spacewire") with performances similar or better to the H2-RG + Sidecar system. The chosen approach was deeply influenced by the on-going definition of the Euclid mission at that time, with the rather optimistic goal of potentially using the newly developed system as backup to the whole H2-RG +SIDECAR from Teledyne or for one of the two elements. The plan has therefore targeted the development of a Large Format array ("LFA") detector as well as a dedicated ASIC controller with specifications tailored to Euclid.
For the LFA, 4 phases were considered:

- Phase 1: demonstration of material capabilities with respect to the parameters given in table 2 with strong emphasis on dark current and quantum efficiency.
- Phase 2: prototype array with respect to further detailed specifications, the main one being presented in table 3.
- Phase 3: full size array 2k x 2k
- Phase 4: optimized full size array up to TRL6 or higher

For the LFA controller, a 2 phase approach was taken:

- Phase 1: building blocks functional ASIC and tests at cryo temperature (77K)
- Phase2: full scale optimized ASIC within specifications.

3.3.1 Large Format Array (LFA)

The phase 1 and 2 were organized as 2 TRP parallel competitive contracts, SELEX-UK/ATC[18] (UK) on one side, and CEA/LETI- CEA/IRFU-SOFRADIR (FR) on the other side[†]. The driving parameters for the material exploration in phase 1 are recalled in table 2. Selex MOVPE (Metal Organic Vapor Phase Epitaxy) material (n-type absorber layer, MCT CdTe buffer layers and GaAs growth substrate) was hybridized to an existing 24 μm pixels in a 320 x 256 CMOS readout circuit (referred as "SWALLOW") with source follower per detector (SFD) topology. A minimum dark current of 0.1 e/s at 80 K and a QE of 74 % in H band[‡] have been reported.[19] Much lower QE value for the blue end of the spectrum were measured. At the end of phase 1, with its own funding Selex has further investigated different process variations, among which dry versus wet etch, as well as

[†]At the beginning of phase 1, QINETIQ(UK) was also selected as a third company but activities were stopped due to the company business re-orientation.

[‡]centered on 1.64 μm with cut-on at 1.47 μm and cut-off at 1.77 μm at 80K

Parameters	Values	Remark
Operating temperature	$80 \leq T \leq 140$ K	
Cut-on wavelength	0.8 μm	
Cut-off wavelength	1.9-2.0 μm	50 % of QE max
Dark current	0.5 $fA.cm^{-2}$	At 100 K
Quantum efficiency	$\geq 80\%$	Over the wavelength range with AR coating.

Table 2: Main parameters of the LFA phase 1.

composition gradient. The goal to bring the absorption within one diffusion length of the junction could however not be achieved .
For CEA/LETI, different growth processes and diode structure were explored: (Liquid Phase Epitaxy) n/p and MBE (Molecular Beam epitaxy) with p/n diode, using an existing 15 μm , 384x288 pixel readout circuit based also on a SFD (Source Follower per Detector). Cut-offs of 2.0 μm and 2.5 μm were processed. Dark current of 0.06 e/s at at 60 K were measured for a p/n MBE growth structure with 2.03 μm cut-off and flat photo-response with typical QE of 70 % have been reported by CEA/IRFU.[20] The 2.5 μm cut-off material performances were still 2 orders of magnitude higher than demonstrated by US manufacturers. The comparison between the different diodes structures and growth process have confirmed that at lower temperatures, the behavior is not the one associated to diffusion current from the absorbing layer but rather by generation-recombination in the depletion layer, with an important role of the surface passivation and material quality.
For both Selex-UK/ATC and CEA/LETI- CEA/IRFU-SOFRADIR, a lower limit of the dark current seemed achievable. It was therefore decided to keep the competition in phase 2, with specifications following the Euclid Near Infrared Spectro-Photometer (NISP) instrument needs at that time as recalled in table 3. One important aspect of phase 2 was also to assess the overall industrialization capabilities, in particular the identification of a clear path toward a 2k x 2k format. At the time of writing of these lines, the core phase 2 has been completed

Parameters	Values	Remark
Format	512 x 512 minimum	
Pixel size (μm)	15 x 15	
Operating temperature	≥ 100 K	
Cut-off wavelength	≤ 2.3 μm	50 % of QE max, operating wavelength range (0.9-2.1 μm)
Dark current	0.1 e/s	Operating temperature
Quantum efficiency	$\geq 70\%$	Over the wavelength range with AR coating.
Total noise	≤ 9 e- rms	for 600 seconds integration time with Fowler-32 sampling
Number of outputs	4/8	

Table 3: Main parameters of the LFA phase 2.

(with the same actors as during phase 1) and an extension of 6 months has just been granted in order to solve the problems identified so far.
Selex has managed to produce a 1280x1032 (1276 x 1024 active pixels) SFD based array (referred as "ME930"). The ROIC performances are in line with expectations in terms of noise, showing a maximum charge handling capacity of 235 ke- (tested) and a linear full well (3%) of 75 ke- for a typical conversion gain of 6 μV/e- (without MCT). The array was tested down to 80 K, with typical power consumption of 33 mW for 4 output mode. Preliminary radiation tests (under Selex own funding) were carried out, revealing a very promising behavior, in particular with respect to the digital library. The dual gain capability by use of a switchable ballast capacitor

is operational. The ROIC shows however one of the output, not always the same (with and without MCT hybridized), with higher noise than the 3 others, the effect is being investigated.
As far as MCT is concerned, different growth were attempted based on the lessons learnt from phase 1. It was however not possible to reproduce the very good QE result of phase 1 in H band and no improvement in the blue end can so far be reported, despite flatter responses in J-H and K bands. An average dark current of ∼0.43 e/s was measured on the matrix 2605-4 (with cut-off of 2.17 μm). The ROIC was designed to be low glow but tests at UKATC have not yet been carried out to assess this point. The phase 2 extension will aim at completing the remaining tests (cross-talk, intra-pixel uniformity, persistence...) and will investigate a new alternative for the MCT thinning step in order to improve QE. Additionally, a 2.5μm cut-off growth will be performed to evaluate the improvement on the thinning due lower x composition in the MCT.
In terms of industrialization capability, Selex offers a straight path to the 2k x2k format (already achieved within the frame of another ESA contract, see section A.2). In terms of packaging, a short study has been carried out within the frame of the contract and following a separately funded collaboration with e2V, a 3 side close buttable package (3 mm gaps between active area on 3 sides) has been designed and manufactured to accommodate the phase 2 ROIC, this is seen as an essential industrial step.
For phase 2, CEA/LETI has focused on MBE (Molecular Beam Epitaxy) p/n with a SFD based 640 x512 newly

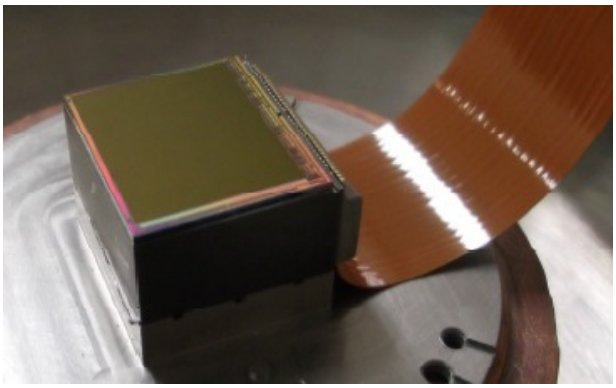

Figure 3: Newly developed close-buttable package with the ME930 ROIC (Courtesy of Selex & e2V)

designed readout circuitry (referred as "CL103"). THE ROIC has 8 outputs, a nominal readout rate of 112 kpixels. Several types of test pixels (pixel capacitance, leakage current, IPC pixels[§]) are available. The ROIC pixel capacitance alone was evaluated to 5.5 fF.
Two different types of diode passivation , two different types of metallization as well as 3 different diode geometries were addressed. Four wafers (PV3261, 62, 63 and 64) of respective cut-off 1.97, 1.9, 2.02 and 2.03 μm were processed, i.e. below the specifications. It is worth mentioning that none of these devices is thinned, i.e., the CdZnTe is still present. Thinning is an additional step which will be considered in the future to lower the cut-on into the visible and to prevent spurious cosmic ray detection in the CdZnTe. PV3261, 63 and 64 have showed excessive surface leakages between neighboring diodes. This was made obvious in particular via spotscan mapping experiment carried out at CEA-LETI. This is likely to be due to a technology accident during the passivation process. Four devices from PV3264 were delivered to CEA-/IRFU, the device CH1318 was in particular tested in depth. The PV3262 wafer showed on the other hand a more standard behavior in terms of coupling with QE in excess of 70 % and 2 devices could be handed over to CEA/IRFU for detailed testing, more attention was given to the device CH1314 which has the 12 diode variants, each variant with a strip of 640 x43 or 44 pixels.
Component CH1318 tests confirmed the strong coupling between diodes with values up to 30%, the dark current at 100 K was measured as 16 times above specifications, it was however possible to record an average value 0.29 e/s at 30 K. For component CH1314, one of the 3 geometry types of diode was not functional, however the operability of the 2 other types is very high. At 100 K , the dark current is 20 times above specifications and the specifications is only met at 50 K. The inter-pixel capacitance measurement revealed that one of the

[§]The CL103 ROIC has 96 pre-defined pixels which can be kept under reset while other pixels integrate light

variants is clearly better. The correlated Double sampling (CDS) technique did not seem to be operational for this device while up the ramp and Fowler are. Overall, some of the parameters are not yet within specifications, this may be linked to the technological accident mentioned previously. The extension granted recently will help answering this question with a new MBE production, besides a direct comparison to p/n Liquid Phase Epitaxy (LPE) material will be made giving the complete picture of state of the art performances MCT for NIR devices at CEA-LETI/SOFRADIR. In terms of industrialization capabilities, SOFRADIR has already manufactured a 1280 x1024, 15 μm pixel arrays (Jupiter MW) and more recently the NGP (see section A.2), some of the challenges for larger devices are currently being addressed. The LFA phase 2 has therefore not yet reached a

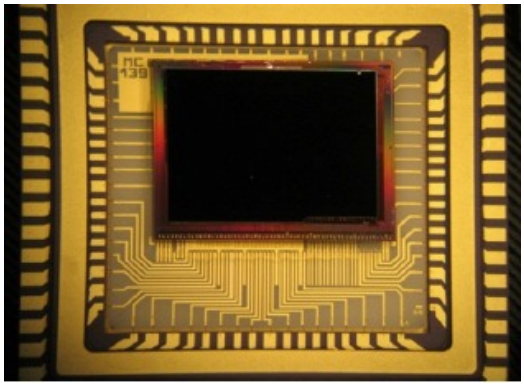

Figure 4: P/n MBE growth device based on the CL103 ROIC

conclusion, delaying the start of phase 3 which should lead to a final product, available to the whole community. The funding for phase 3 is approved (TRP), and we hope to start the activity by Q1 2015. The phase 4, based on a CTP, will bring the device to TRL6. Ideally such device could be part of a payload on a M5 mission, for which TRL6 is required by 2020.

3.3.2 LFA controller

The interest of an ASIC (Application Specific Integrated Circuit) capable of generating bias voltages, clock signals as well performing high performance digitization on multiple channels has been demonstrated for a long time for large mosaic focal planes. The SIDECAR (System For Image Digitization, Enhancement, Control and retrieval) is currently the reference and has been widely used in Astronomy applications, on ground and in space, usually coupled to the H2-RG device (JWST, Euclid...) but not only with the particular example of the Advanced Camera for Surveys (ACS) on board Hubble where the ASIC was used to control CCD[21].
The phase 1 LFA controller activity started in April 2012 with the Caeleste (Belgium) company as prime contractor,with EASICS (belgium) and SELEX (UK) as sub-contractors. As mentioned in the introduction, the genesis of the LFA controller started with the aim of providing a European backup to the SIDECAR for Euclid, therefore compatibility with the H2-RG interfaces and performances were part of the original specifications. Additional features like spacewire[22] interface capabilities, in particular the implementation of the Remote Access Memory Protocol (RMAP) were added to solve some of the system issues encountered during the Euclid mission assessment. The main specifications of the phase 1 prototype controller are given in 4. To the complex micro-controller approach of the SIDECAR, a more limited yet flexible nested loop sequencer type approach was preferred. The sequencer controls the internal ADCs and digital inputs readouts, sets the Analog to Digital Multiplexers and initiates the data transfer. The sequencer is based on several blocks:

- The series memory which contains 512 series of 16 pairs of (delay ID, event) as well as a repeat count. The ID can refer to a defined event or to another series
- The sequence generator which parses the series and generates a sequence of event-delay pairs
- The stack which allows 8 levels of nested series
- The event memory which associates an event to all information required to control the clocks, ADCs...

Parameters	Values	Remark
Operating temperature	77K to 398 K	
Current consumption	$\leq$ 40 mA	With All ADCs operating at 100 kHz sampling
Minimum TID (Total Ionizing dose)	50 krad	
SEE threshold	60 $MeV.cm^2.mg^{-1}$	Immune to Single Event Latchup
Digital interface (data and control)	Spacewire	Up to 200 MHz. SPI is also implemented for control.
Number of regulated power supplies	4	
Number of programmable voltage reference outputs	8	10 bits flash DACs
Number of clock outputs	32	up to 10 MHz
Number of digital control outputs	8	
Number of digital control intputs	8	
Number of Analogue inputs	16	4 processing chains with a MUX4 on each chain. DAC offset compensation
Number of digital control outputs	8	
ADC resolution	16 bits	
Analogue input referred noise	$\leq$ 0.25 bits with gain 1	
Sampling rate	100 kHz per input	Goal of 200 kHz
Additional HouseKeeping inputs	4	16 bits , 100 kHz, relaxed input referred noise. Built in temperature sensor

Table 4: Main specifications of the LFA controller

- The event controller which executes the event receives from the sequence generator (via a dedicated FIFO) at a given time with the associated inputs from the event memory and from a correspondence table between delay ID and true delay.

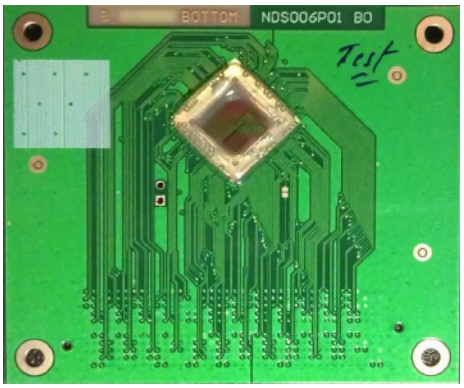

Figure 5: The LFA controller prototype on its test PCB.

The chosen technology is UMC180 nm mixed signal (1-poly 6-metal). One of the main advantage of this technology is the availability of the Design Against Radiation Effect (DARE)[23] library which provides digital standard cells (tested). The activity is close to completion. Room temperature tests have been completed using

the ASIC mounted on a PCB (so called "Chip On Board", COB) as shown on figure 5 and cryogenic tests were carried out at SELEX on a specific low temperature test board. The preliminary results show that the device is fully functional down to cryo temperature, the detailed performances are under review. It is worth mentioning that a parallel activity is also run by ESA (with slightly relaxed specifications, in particular for the ADC) with the company IDEAS[24] (Norway).

3.4 Visible

The recent and future activities in the visible optical wavelength range are addressing both CCD and CMOS technologies. CCD are almost exclusively associated to Astronomy missions while CMOS imagers sensors (CIS) are becoming more a target of choice from planetary type missions.

3.4.1 N-channel CCD

For CCD with standard N-channel technology , the recent selection of the PLATO mission as M3 (see section 2.1) has triggered the preparation of the qualification program of the CCD270 which should start very shortly at e2V. One of the main challenge of PLATO is the capability to manufacture the 34 telescopes (120 mm pupil diameter) which are presently foreseen to achieve the scientific goals. Each telescope has a 2 x 2 focal plane arrays based on the CCD270 for which 2 variants are manufactured as can be seen on figure 6. The full frame variant will be used in the so called 32 "normal" cameras, while the frame transfer version is used in the 2 "fast" cameras used for fine attitude control. A total of 136 Flight models (plus spares) are therefore required.
The main features of the CCD270 are its size of 81 mm x 81 mm of active surface made of 4510 x4510 pixels of 18 μm pitch, a full well capacity of 900 ke- minimum and a noise which shall be below 28 e-rms at a frequency of 4 MHz. The pre-development activities carried out before the mission selection have enabled E2v to:

- evaluate the risk associated to the production[25]
- consolidate the performances with respect to the initial specifications by fully testing 15 devices (Front illuminated, Back illuminated, Full frame, Frame Transfer), delivered to ESA. These devices will be used by the PLATO consortium to manufacture and test an engineering model of a telescope and also for further tests by the Agency (see section 4.1).

The qualification program will essentially follow a similar approach than for Euclid, ie based on tailoring the Escc9020[26] . The production of a sufficient number of devices to start the qualification flow as well as the development of a new characterization camera at e2V are the first challenges to be addressed. This phase shall be completed before the adoption (see section 2.1) of the mission in February 2016. It is interesting to note that to avoid the use of the large CCD270 for tests like radiations tests, a smaller version of the device, called CCD280 is manufactured on each wafer, the qualification flow will aim at demonstrating the equivalence of the two for the relevant parameters. A similar approach was used on GAIA and initially on Euclid (see section 3.4.2).
ESA is also responsible for the procurement of the Engineering (EM) and flight models (FM) of the CCD 47-20

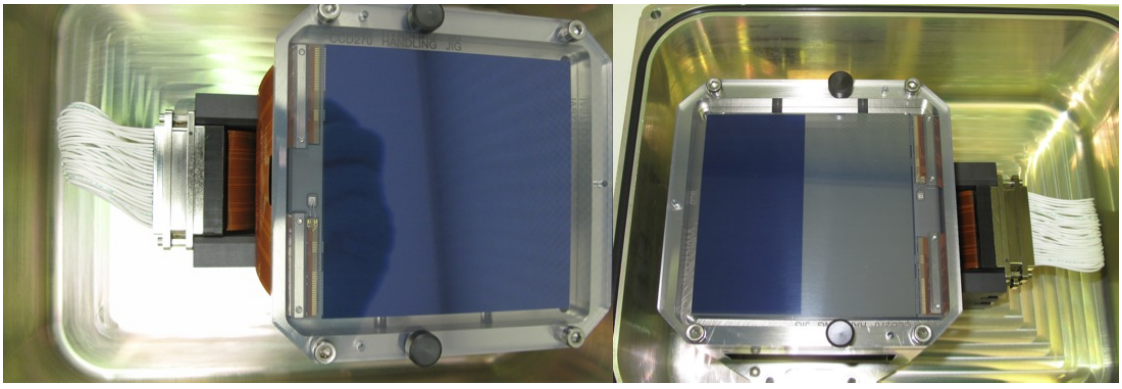

Figure 6: The CCD270 2 variants for PLATO: full frame on the left handside, frame transfer on the right handside.

for the CHEOPS[1] mission. Due to the very short development time of the mission, the procurement has been initiated in July 2013 when the program was in phase A. The activity is organized in 2 phases, phase 1 for the EM and phase 2 for the FM with standard screening, lot acceptance and radiation tests flows. The activity is proceeding nominally.

3.4.2 P-channel CCD

The p-channel activities have been initiated during the assessment phase of the Euclid and PLATO missions. The e2V CCD203 (n-channel) was initially proposed by the Euclid consortium as baseline. The CCD204, a smaller version of the CCD203 used for radiation testing, including charge injection, was used immediately for test in order to assess the impact of proton irradiation on shape measurements and optimum operating temperature of the device[27].

No p-channel devices were available at that time with a sufficiently high TRL to be considered for Euclid, however the potential known improvements of p-channel over n-channel from previous studies[28], were seen as worth investigating. Discussions on the ability to establish a proper comparison[29,30] between n and p were also taken into account. It was therefore decided to have a p-channel version of the CCD204 manufactured, prefiguring potentially a p-channel version of the 203 for Euclid and allowing direct and unambiguous comparison with the twin n-channel. Pre-irradiation performances of the p-CCD204 indicated CTI values similar to the n-CCD204 below 173 K, however the dark current was approximately a factor of 2. Cosmetics quality of the p-CCD204 were not yet completely satisfying with performances better than n-channel for the best devices but considerably worse for bad devices.

Using the optimized operational parameter (clocking, temperature) for the n-channel, the p-channel improvement was limited if non-existing in terms of radiation hardness. By that time, using p-channel for Euclid was not possible anymore due to TRL and programmatic constraints however the need to push further the exploration of the p-channel 204 operation was acknowledged and a dedicated test activity was funded by ESA. The activity has been initiated in September 2013 with Open University[31]. The activity aims at at a detailed investigation of the p-CCD204 performances (CTI, dark but also PSF, MTF...) with definition of an optimised operational point. Irradiation warm and cold will also be part of the program. The device selection is now completed and the activity is at the test readiness review level. The results of the program will be used to trigger (or not) a follow on activity aiming at designing and manufacturing a full scale p-channel device integrating all the lessons learnt.

3.4.3 CIS

While CCDs are still recognised as the work-horse detector for demanding scientific applications in the visible waveband, CMOS image sensors (CIS) continue to improve and hold many promises for improved operation with regard to read-out speed, flexible windowing, radiation tolerance, ease of interfacing and power consumption. ESA has a continual programme of development in this area, including the exploration of a completely European sensor (but not to the exclusion of all else), where design house, foundry and post-processing facilities are all located within ESA member states. Part of the ESA remit is to further European technology capabilities and support independence.

Under this umbrella, the Agency has been investigating the possibility to develop a completely European supply chain for high-performance CMOS image sensors, including the foundry. A well-attended workshop was held in 2010 at ESTEC, with participants from design-houses, foundries, industry and end-users, where the overwhelming consensus was that such a path be pursued. Consequently, the Agency put in place a number of development activities to investigate and stimulate the design and manufacture of a space-worthy CIS within Europe. These activities were grouped together under the names of European Low-Flux and European High-Flux CIS, with broad aims of targeting Astronomy and Earth Observation type applications respectively.

Unfortunately, in between the workshop and the initiation of the development activities, the foundry landscape within Europe changed significantly, reducing the number of possible options. However, the High-Flux sensor development is well underway (see section A.3) , while the Low-Flux sensor activity is due to start in Q2 2014.

3.5 Micro-calorimeters for X-ray applications

Various studies (XEUS, Constellation-X, IXO, ATHENA) for future X-ray missions beyond XMM-Newton and Chandra have baselined cryogenic instruments with TES-based microcalorimeter arrays for time resolved imaging high resolution spectroscopy[9]. With the selection of the science theme "the hot and energetic Universe" for L2 the second Large-class mission in ESAs Cosmic Vision science programme which is expected to be pursued with an advanced X-ray observatory, such an instrument is likely to be realized. Typical requirements for its detectors include: FWHM energy resolution ∼2.5 eV, energy range 0.2-10 keV, pixel size 250 μm, array size up to 4000 pixels. ESA will start a new activity for further development of TES technology for such applications by the end of 2014. It is important to note that eventually such technology will be very likely part of a nationally funded payload, ie not under responsibility of ESA, however due to its criticality and impact at system level (e.g. cooler, under ESA responsibility), the technology is covered now under the CTP program (see section 2.1).

3.6 Gamma ray detectors

Three activities focusing on gamma ray applications have recently been completed successfully. The first one is based on the development on 3D position sensitive CZT (Cadnium Zinc Telluride) detector, targeting future hard X-rays applications.
The other two activities are basically focusing on scintillators. In particular, new developments in lanthanum halide scintillators[32] have resulted in the availability of high performance, large-volume gamma-ray detectors. Current detector modules use photomultiplier tubes and although they have high energy resolution, they also suffer from low quantum efficiency, have large volume and mass and require high bias supplies. Alternative technologies are now becoming available in the form of the solid state detectors and the Agency has been investigating their capabilities in the frame of a series of technology development activities. In addition, potential future high-energy astrophysics missions such as gamma-ray observatories[33] have demanding requirements in terms of spectral, temporal and spatial resolution and will require hundreds or even thousands of individual detector arrays. As a complement to the on-going detector development activities, ESA is also pursuing the development of a custom ASIC to support the read-out and operation of such a large-scale instrument.

3.6.1 3D position sensitive CZT detectors

This activity was led by DTU Space(Danemark) and aimed at developing and testing a high energy 3D position sensitive CZT detector with energy range 20-2000 keV, mm position resolution and sub percent energy resolution at 662 keV.

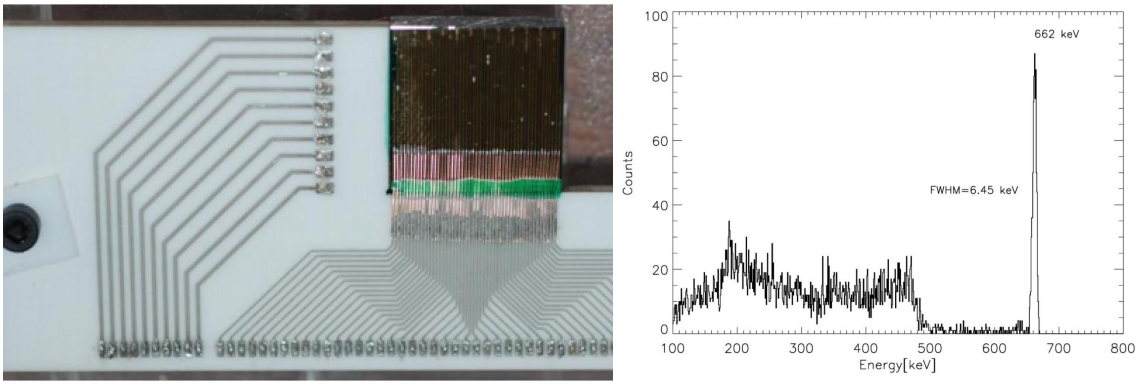

Figure 7: On the left: 3DZT prototype developed by DTU (CZT detector size is 20 mm x 20 mm x 5 mm). On the right: Energy spectrum of ^{137}Cs measured in a detector of 1 mm^3 volume close to the cathode plane of the 3DCZT detector.

The technology is based on the so-called CZT Drift strip detector (already developed by DTU Space) enhanced by a novel readout scheme enabling the 3 D position sensitivity. Such detector offers excellent spectral performances, close to Germanium, without some of the cryogenic constraints. The biasing and readout structure

of the device is such that the signal on the anodes are proportional to the photon energy, benefiting directly of the poor mobility of holes as opposed to the good drift of electrons in the CZT. The anodes provides also position information along one axis while the other axis position is determined thanks to the "Depth of interaction technology"[34].
The position resolution as well as energy resolution were characterized at the ESRF (European Synchrotron Radiation Facility). Figure 7 shows the excellent energy resolution obtained with a ^{137}Cs source, less than 1%. The overall performances achieved are extremely promising for future hard X-ray rousing telescopes and Compton Camera telescopes.

3.6.2 Silicon drift detectors

Silicon drift detectors (SDD) are now relatively mature technology with proven performance, most commonly applied to direct X-ray detection activities[35]. However, they are also capable, low noise detectors for use in the UV-visible waveband. Based on this, the Agency has pursued the development of custom SDD arrays, optimized for use at the peak light output wavelength of LaBr3 (Ce) scintillators, through an Italian consortium. Led by Politecnico di Milano, the consortium have successfully designed and manufactured arrays of 8 mm square format SDD detectors[36]. Arranged as a group of 3 x 3 SDDs, a single array directly supports the read-out of a 1" LaBr3 crystal. Further, due to the modular design, the arrays can also be tiled and have been successfully demonstrated in 6 x 6 format as the detector in a 2" crystal gamma-ray detector. Each 3 x 3 SDD array is mounted on a custom ceramic circuit board with pre-amplifiers in die form mounted on the reverse. The required number of detector modules are then mounted onto a baseplate to provide a readout for a 1" (1 detector module), 2" (2x2 detector modules) or 3" crystal (3x3 detector modules). The baseplate is then assembled to the Peltier cooler and scintillator crystal modules as shown in Figure 8.

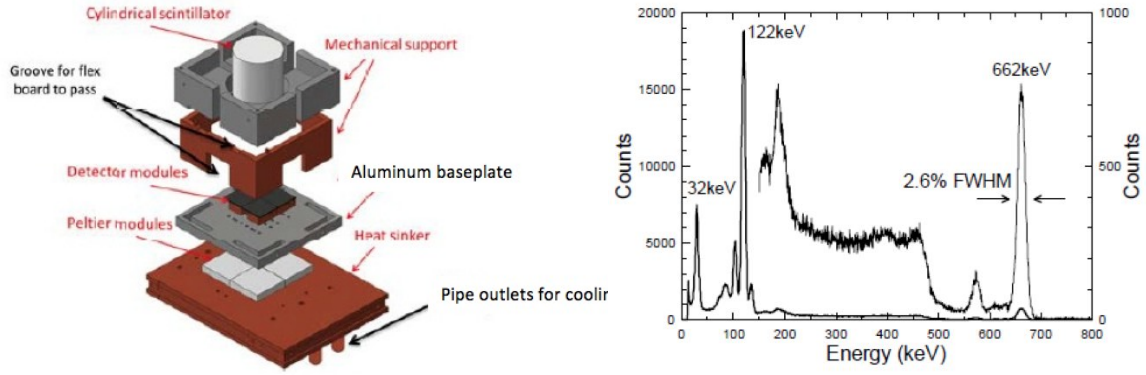

Figure 8: On the left: Exploded view of SDD detector module, including thermoelectric coolers and scintillator crystal. On the right:Energy spectrum of ^{57}Co and ^{137}Cs measured simultaneously with SDD coupled to LaBr3 crystal.

Gamma-ray source measurements using modules equipped with 1" and 2" LaBr3(Ce) crystals have demonstrated very high performance (see figure 8), opening the way for future application of such detector modules.

3.6.3 Silicon Photomultiplier Development

The major aims of the Agency's Silicon Photomultiplier (SiPM) programme have been:

- to develop a SiPM device architecture with peak photon detection efficiency corresponding to the emission spectrum of the lanthanum halide family of scintillators i.e. 350 - 400 nm
- to assess the reliability of the technology for space application through a rigorous test campaign.

The detector developed within the programme consists of a p-on-n Geiger mode Avalanche Photodiode (APD). The device structure and doping profile have been optimized to ensure optimum efficiency in the targeted spectral range keeping in mind that 99.5% of 350 nm photons are absorbed within 50 nm of silicon. Several pixel sizes

have been produced with a size of 6 mm x 6 mm pixel consisting of 18980 individual 35 μm diameter APDs (microcells) being selected for producing a packaged device suitable for performance and reliability testing. The final device consists of an 8x8 array of 6 mm square pixels arranged in a hermetically sealed ceramic package as shown in figure 9a. In this package configuration, the anodes and the cathodes of the individual pixels are joined together, and the readout is achieved using a transimpedance amplifier over the common anode and common cathode. This single readout approach was chosen in light of the reference application which is gamma-ray spectroscopy applied to planetary surface composition mapping as in the case of the Mercury Gamma-Ray and Neutron Spectrometer (MGNS) instrument onboard the ESA Bepi Colombo mission. The devices are manufactured by SensL, Ireland and for detailed performance information, the reader is referred to http://sensl.com/downloads/ds/DS-MicroBseries.pdf.

The critical performance metric applied to the devices was the full width at half maximum (FHWM) energy

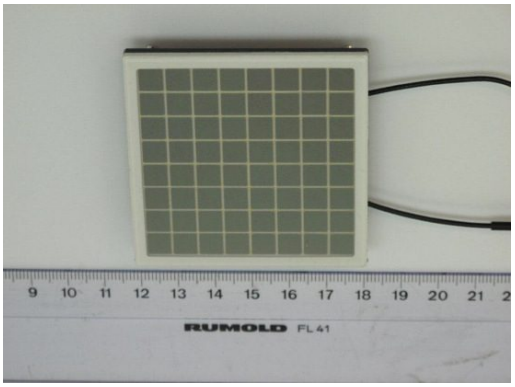

(a) Packaged SiPM array consisting of 64 6 mm x 6 mm pixels.

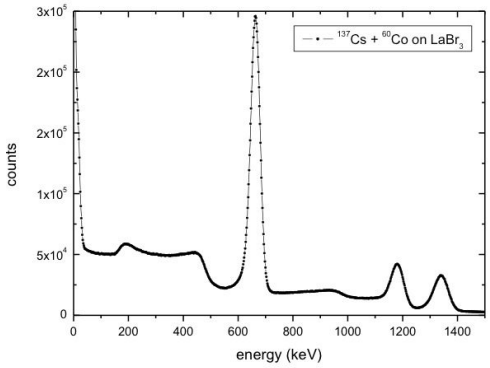

(b) Gamma-ray spectrum of ^{57}Co and ^{137}Cs recorded with a 50 mm diameter LaBr3 scintillator with SiPM readout. A preamplifier shaping time of 0.5 μs and integration time of 300 s.

Figure 9: Newly developed Silicon Photomultiplier and associated performance demonstration.

resolution of the ^{137}Cs 662 keV line. Figure 9b shows a typical spectrum obtained at room temperature and with the device biased at 2V above the breakdown voltage of 23 V. Note that the breakdown voltage is defined as the voltage at which a 6 mm die passes 100 nA reversed bias current in dark conditions. The spectrum was recorded with a 50 mm diameter Cerium-doped Lanthanum Bromide (LaBr3) scintillator which was positioned directly on top of the detector package. ^{137}Cs and ^{60}Co sources were in turn placed directly on top of the scintillator crystal. LaBr3 has a high scintillation yield of 63 photons/keV and the scintillation light emitted is in the wavelength range 340 nm-420 nm. It typically provides the best energy resolution of all scintillating crystals when used in combination with blue sensitive detectors. The best recorded energy resolution for the SiPM readout LaBr3 was observed to be 4.5% at 662 keV. Although somewhat higher than the best reported resolution of 3% for a photomultiplier readout, the value achieved for the SiPM demonstrates its potential as a low resource, low voltage, rugged solid state alternative to the classical technology. Following the verification of the detector performance the devices, at both pixel and package level, were subjected to a series of environmental and endurance tests specified to assess the technology for space application. At pixel level 240 devices were subjected to 1000 hour high temperature operating life (HTOL) at 125 ^{o}C. The key opto-electronic performance indicators of dark current, breakdown voltage, photon detection efficiency and gain were monitored. No functional or parametric failures were observed and all devices were within specification (e.g. gain within 4% of pre-test level) following the HTOL test. At package level the devices shown in figure 9a were subjected to temperature cycling, mechanical shock, vibration, moisture shock and operating life testing in accordance with the relevant MIL standards. In general, the opto-electronic performance of the devices following testing was found to be satisfactory. All 4 devices under test successfully passed the temperature cycling, mechanical shock and vibration testing. The energy resolution of the packaged devices was measured before and after all testing and a slight degradation was noted following the 2000 hour operating life test with the mean resolution of the four packaged devices under test

increasing from 5% to 5.2% (FHWM at 662 keV). The test was conducted at 125 ^{o}C and it is thought that some changes in the optical transmission of the package cover glass and or changes in the optical absorption of the protective polymeric layer on the pixel surfaces may have occurred. It is also noted that 2 of the 4 devices failed the fine leak testing following the moisture stress testing indicating that further work is required to improve the quality and yield of the package sealing process.

3.6.4 Custom ASIC for SiPM read-out

A custom ASIC development activity has been initiated with the aim of prototyping the low-power, high-density support electronics that will be necessary for any future gamma-ray astronomy missions employing solid-state detector modules.

3.7 Long-term technology directions

A number of interesting options exist within the infrared regime for applying emerging technologies. ESA recently commissioned a study into the status of detector technologies for use in the thermal infrared. The study looked at both thermal and photon detectors. While μbolometers were recognized as having a role in certain types of space missions, Type-II Superlattice detectors were identified as very promising technology, especially as a performance matching competitor to MCT in the LWIR and VLWIR. The Agency plans to launch a technology development activity in this area later this year. At the other end of the IR waveband, APD arrays are starting to find application (e.g. wavefront sensors) and ESA intends to launch a study into the potential use of this technology in photon-starved applications.

4. PAYLOAD TECHNOLOGY VALIDATION ACTIVITIES

The Payload and Technology Validation section in the Science and Robotic exploration directorate is providing support to present and future missions at different step in their lifetime. The main activities are:

- support to SRE-F (Future missions): the main goal is to validate the technology for future mission in order to de-risk the overall program before the mission adoption (occurring at the end of phase B1). The synergy between the mission study team, the Technology development activity technical officer and the test team is optimized. A first example was Euclid and the CCD273, a more recent one is PLATO....Technology validation for the long-term is also addressed, NIR activities and its "Photon to spw" (as developed in section 3.3) activities are in first line.
- support to SRE-P (Projects): projects in development are requesting specific tests to be performed to insure control of some performances under ESA responsibility or affecting items under ESA responsibility. Euclid is now in that configuration.
- support to SRE-O (Operation): the activities are dedicated to mission in operation with essentially cross-validation on ground of effects observed on instrument on board. A typical example is GAIA.

With limited resources, support is also given to SRE-S (Science) scientists with the implementation of small research programs with internal funding, the latest examples are the DECA (Descent Camera) camera delivered to the EXOMARS project and the on-going SPOSH (Smart Panoramic Optical Sensor Head program[37]).
Due to the long-term heritage of the Science and Robotic Exploration laboratories, most of these activities are presently focusing on detector technology, however on the long-term, the scope will become broader.

4.1 Future mission technology

Experimental support at ESA to future missions has proven to be essential during the study phase of the Euclid mission. Indeed, in parallel with the mission phase A/B1, a specific pre-development of the CCD273 at E2v took place for the VIS instrument focal plane mission. The CCD procurement being the responsibility of ESA, it was decided to ensure experimental validation of the CCD273 (and the CCD204 before) as early as possible in parallel with industrial activities[27] and the Consortium activities.
For PLATO and CHEOPS CCDs (see section 3.4.1), the same level of support has already been initiated[38] and will intensify in the future in particular for PLATO for which two main items need to be addressed before the mission adoption: radiation, impact of the coupling between the motion of the star due to spacecraft jitter and the CCD Photo Response Non Uniformity on the extremely tight photometry budget.

On the longer term, a complete validation plan of the industrial activities detailed in section 3.3 has been set, aiming at a full system validation LFA + LFA controller for the M5 mission, using tests facilities developed for the SIDECAR+H2-RG tests[39].
Support for the future L2 missions will also be envisaged, the exact scope is currently under discussion.

4.2 Projects in implementation

The support to project in implementation is essentially focused on Euclid:

- The initial CCD 273 activities[40,41] have paved the way to detailed testing of the impact of radiation on shape measurement[42,43] using photolithographics masks with sample galaxies projected onto the CCD.
- The HAWAII testing[39,44] initiated during the assessment phase of Euclid have progressed slowly but should reach soon a cruising speed. The tests are focused on remanence and sub-pixel response impact on photometry. A full SCS (Sensor Chip System), ie H2-RG + flexi+ SIDECAR from the latest Euclid production batch at Teledyne will be used soon. Another H2-RG (#224, 2.5 μm cut-off) has already been tested and is used to commission all facilities.

4.3 Mission in Operations

This specific type of activity has been inaugurated with GAIA. One of the key elements of GAIA is obviously the focal plane with the CCDs and control electronics (PEM: Proximity Electronic Module) and a very large effort has been made well before launch to investigate the effect of radiations on the overall astrometric performances and define adapted mitigation techniques (diffuse optical background, charge injection, modelling...). A dedicated test bench, able to simulate the motion of stars (due to the GAIA spacecraft spin) on the CCDs operated in TDI (Time Delay Integration) mode, was developed at Airbus DS (formally Astrium). At the end of the industrial phase of GAIA, the bench was delivered to ESA with the goal of helping the inflight commissioning and further on in the mission having the possibility to provide a ground reference point.

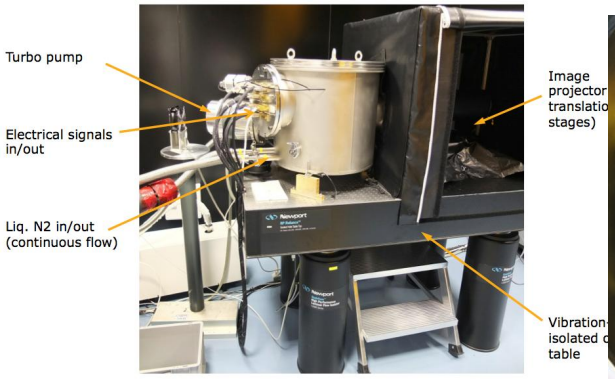

(a) The test bench with optical table, translation stage reproducing the star motion on the GAI focal planes, an illumination system and the cryostat.

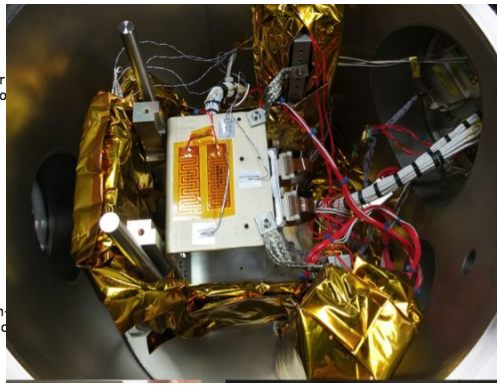

(b) Closer look on the GAIA cryostat which contains 2 CCDs and associated PEM.

Figure 10: The GAIA CCD test bench at ESA.

Several test campaigns have been successfully performed so far, the analysis of the results is performed by the GAIA operation team. The bench will remain active as long as required by the operation team.

5. CONCLUSION

A detailed status of the present and future detector activities of the European Space Agency for the scientific program, so called "Cosmic Vision", has been presented, covering a very wide range of wavelengths, from LWIR to gamma rays. The associated technology program benefits also from other ESA programs, in particular Earth

Observation and a tight link is maintained to allow a consistent approach in Europe.
CCD, CMOS imagers, NIR, MWIR-LWIR detectors and associated ASIC controllers, TES and other Silicon Photomultipliers are being developed to answer the future scientific needs. The European Space Agency needs these technologies in Europe with state of the art performances to propose world-class science missions while optimizing the geo-return.

APPENDIX A. EARTH OBSERVATION PROGRAM DETECTOR TECHNOLOGY STATUS

In parallel with the developments for Astronomy-like missions discussed above, ESA is also undertaking a series of strategic detector developments targeted at future Earth Observation missions, in both the infrared and visible wavelengths. The technology involved and progresses made are usually directly relevant for scientific technology program managed by ESA or for planetary missions nationally funded payloads, typical examples are hyperspectral imagers on board Bepi Colombo or JUICE (Jupiter Icy Moon Explorer).

A.1 LWIR

The Low Dark Current 2D VLWIR detector activity aims at demonstrating, at material level, the possibility to reduce dark current at a given temperature, by proposing innovative designs and improvements of the current MCT detection layer design. It is following a previous development aimed at preparing detectors for the different instruments on board the next meteorological series of satellites MTG (Meteosat Third Generation). Two bands are targeted : LWIR (cut-off 11.5 μm) and VLWIR (cut-off 14.5 μm), the challenge being the dark current density. A summary of the main requirements is given in table 5. No specific Read-Out Integrated Circuit is required to enable to concentrate the development effort at MCT level: the demonstration of material performances is done through the use of existing, not necessarily space qualified, ROIC.

Parameters	Band 1	Band 2	Remark
Cut-on	8 μm	10 μm	Minimum value
Cut-off	11.5 μm	14.5 μm	At operating temperature
Pixel size	15 to 30 μm	15 to 30 μm	
Dark current density	$\leq 10^{-4}\ A.cm^{-2}$ (Goal is $\leq 10^{-5}$)	$\leq 6.5\ 10^{-4}\ A.cm^{-6}$ (Goal is $\leq 10^{-6}$)	
Operating temperature	80 K	55 K	
Detection efficiency	$\geq 60\%$	$\geq 60\%$	
Cross-talk	$\geq 2\%$	$\geq 2\%$	Total cross-talk

Table 5: Main specifications for the Low Dark Current 2D VLWIR detector.

Two parallel activities are on-going with Selex ES (UK) and AIM (Ge) and the demonstrators are currently being manufactured. Results are expected early 2015.

A.2 SWIR

Contrary to many science missions, Earth Observation applications are not photon-starved. In fact the opposite can apply and typical detector requirements include the ability to handle high input fluxes. SNR (Signal to Noise Ratio) is often limited by photon shot noise but the need to measure scenes with high dynamic range also calls for low detector read-noise. Mission demands for high spatial and spectroscopic resolution are the main drivers for increases in detector size and number of pixels and wide-bandwidth operation while all the time continuing to improve the overall detector performance in terms of QE, read-noise dark current etc. To this end, ESA has put in place some particular development roadmaps in support of future Earth Observation missions.

The need for a 2k x 2k pixel detector with high charge handling capacity operating in the 1 - 2.5 μm waveband was identified as part of the ESA Earth Explorer programme (referred as "Large format SWIR"). Consequently the requirements were formulated and the open competition ITT was won by Selex-ES in the UK.
Developing a 2k x 2k detector with pixel pitch between 15 and 20 μm presents a number of challenges in terms of both the Read-out integrated circuit (ROIC) and the hybridization of the PV-MCT layer. As such, the development program was divided into two activities, the first activity aims to design and manufacture the ROIC but limited to a one-quarter area (1k x 1k) PV-MCT hybridization to demonstrate the performance. The second activity aims to complete the development with the manufacture and hybridization of a full 2k x 2k PV-MCT layer.

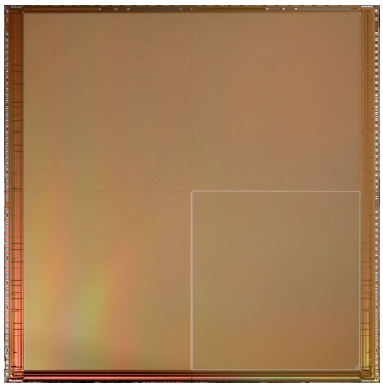

Figure 11: Picture of the 2k x 2k ROIC presently under characterization at Selex.

Parameters	Values	Remark
Format	2048 x 2048 minimum	Reference rows and columns in addition
Pixel size (μm)	17 x 17	
Pixel design	SFD	
Readout	Integrate while Read, snapshot	
Operating temperature	$\geq$ 150 K	
Cut-off wavelength	2.5 μm	
Charge Handling capacity	Gain 1: 100 ke-, Gain 2 : 1 Me-	Design values
Dual gain	Gain 1: 68 e-rms, Gain 2: 109 e-rms	Predicted values
Number of outputs	16	Readout speed 10 MHz/output
Frame rate	40 Hz	

Table 6: Large format SWIR detector specifications.

The first activity is well underway, with the recent delivery of the 2k x 2k ROIC to Selex (see figure 11) where it is undergoing initial characterization. The main specifications of the ROIC are presented in Table 6.

Many Earth Observation missions aim for multi or hyper-spectra images and this typically requires multiple spectrometers and different types of detectors, resulting in associated difficulties of image co-registration. A panchromatic detector with high sensitivity across a wide bandwidth can alleviate some of these problems by accepting input from multiple spectrometers. Electronics interfacing is also simplified if the same type of detector can be used within an instrument. To this end, ESA has undertaken the development of a large format panchromatic MCT hybrid detector with Sofradir in France. The tunable cut-off wavelength of MCT is well known, while the cut-on wavelength is typically limited by the substrate on which the detector is manufactured,

to around 0.9 um. What is important here is that the cut-on wavelength is not limited by the MCT material itself and by thinning the substrate the detector sensitivity can be extended to shorter wavelengths into visible and even into the UV. A first activity with Sofradir[45] demonstrated the viability of this approach with a flat QE measured down to 400 nm for a 2.2 um cut-off detector. Following these results, a second activity, the Next Generation Panchromatic (NGP) detector development was started, also with Sofradir. The aim of this activity was to develop a large-format array with high sensitivity from 0.35 to 2.5 μm.

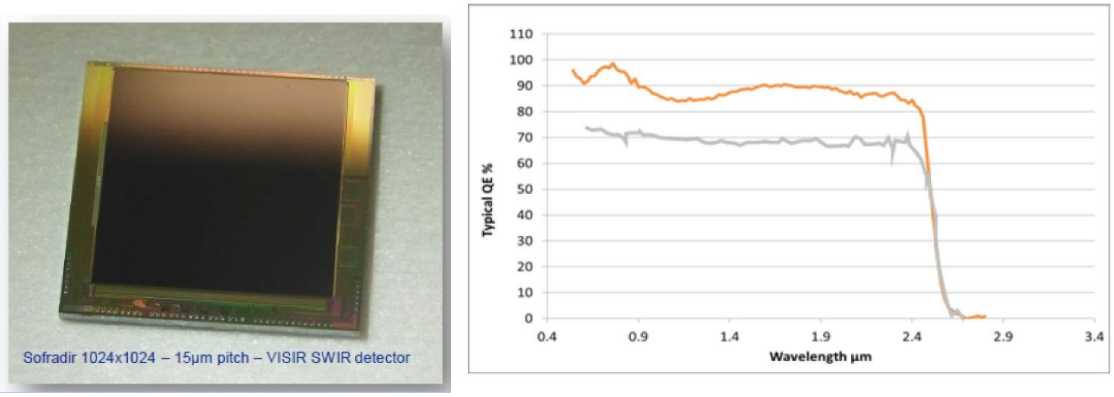

(a) The NGP.

(b) Measured quantum efficiency of the NGP detector: grey without AR coating, orange with AR coating

Figure 12: The Next Generation Panchromatic detector.

Parameters	Values	Remark
Format	1024 x1024	
Pixel size (μm)	15 x 15	
Pixel design	CTIA	
Readout	Integrate while Read, snapshot	
Operating temperature	$\leq$ 170 K	
Cut-off wavelength	2.5 μm	
Charge Handling capacity	680 ke-	Linear range
Read-noise	$\leq$ 140 e-rms	Predicted values
Number of outputs	4	Readout speed 8 MHz/output
Frame rate	30 Hz	

Table 7: Next Generation Panchromatic Detector specifications.

The NGP detector development was successfully completed in 2013, producing a 1k x 1K, 15 μm pitch array based on Sofradir LPE technology. The ROIC uses CTIA pixel topology and incorporates radiation hardening techniques. In addition, a new multi-layer anti-reflection coating was also developed meeting not only the detection efficiency requirements but also providing very low reflectance an important parameter in optical instrument design to reduce straylight and ghost-reflections. Figures 12a, 12b and Table 7 show the measured performances of the NGP detector and the specifications.

A.3 Visible

In order to provide an acceptable alternative to CCDs, CIS need to approach the high-level electro-optical performances offered by their cousin. In particular, QE, dark-current, uniformity and dynamic range. It is clear

from the literature that CIS are making great strides in all these areas but combining all the best performances into a single sensor is still the goal. In conjunction with CMOSIS in Belgium, the Agency is in the process of developing a 1k x 1k, 20 um pitch, back-illuminated CIS. The main design parameters are given in Table 8.

The sensor architecture provides for dual-gain operation with snapshot shutter. Each pixel contains both a

Parameters	Values	Remark
Format	1024 x1024	
Pixel size (μm)	20 x 20	
Pixel design	8T	Dual gain
Readout	Integrate while Read, snapshot	
Operating temperature	240 K	
Charge Handling capacity	Gain 1: 58 ke-, Gain 2: 514 ke-	Linear range
Read-noise	Gain 1: 27 e-rms, Gain 2: 233 e-rms	
Number of outputs	4 or 2	Selectable. 10 MHz output
Frame rate	16 Hz	

Table 8: Back illuminated CIS specifications.

high-gain and a low-gain channel which, in conjunction with the column amplifiers, provide CDS capability. Both gain channels are captured and read-out simultaneously through either 2 or 4 outputs. Post-processing off-chip can then be used to combine the two images if necessary, providing high dynamic range. The detector is manufactured using the Tower 0.18 μm process and is now in its second iteration. The first deliverable arrays suffered from high numbers of hot-pixel clusters that were eventually traced to a combined process/design issue. This was corrected and a second fabrication run performed. The front-side illuminated detectors have been delivered to CMOSIS and are now undergoing initial characterization. An image from one of these new devices is presented in figure 13. Following successful completion of the FSI devices, the back-side processing will be performed.

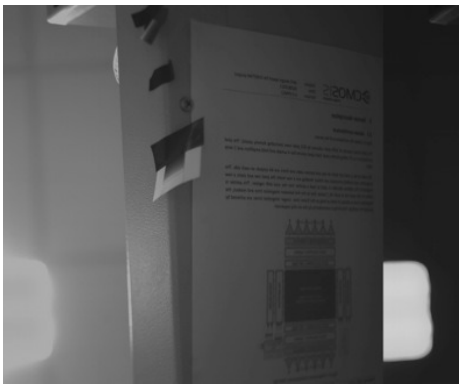

Figure 13: First image from the back-thinned CIS.

In parallel, and as mentioned earlier, the Agency is supporting through a special development program the implementation of a fully European supply chain for CIS manufacturing. The High Flux CIS is part of this strategy with an implementation on two foundries in parallel. The development is led by CMOSIS (Belgium). The IMEC130 nm and the ESPROS (150 nm) have been identified as preliminary foundries. The required performances of this back side illuminated device, summarized in the table 9, have some similarities with the device presented in table 8, the emphasis being placed here on the European flow for the design and manufacturing.

The design phase of the High Flux CIS is on-going, the preliminary design review has been completed, the first prototypes will be ready in 2015.

Parameters	Values
Format	512 x512
Pixel size (μm)	20 x 20
Quantum efficiency	$\geq$50% over [350 nm- 800 nm]
Full well	$\geq$ 500 ke- (dual gain architecture)
Read-noise	50 e-rms (CDS on chip)
Frame rate	40 Hz
Specific features	Global shutter, windowing capability

Table 9: High flux CMOS imager sensor main specifications.

ACKNOWLEDGMENTS

The authors would like to thank Caeleste, CMOSIS, CEA/LETI, CEA/IRFU, SOFRADIR, Selex for their support in the preparation of this paper.
The work carried out by LETI and detailed in section 3.2 has been partially supported by the "LabEx FOCUS ANR-11-LABX-0013".

REFERENCES

1. C. Broeg, A. Fortier, D. Ehrenreich, Y. Alibert, W. Baumjohann, W. Benz, M. Deleuil, M. Gillon, A. Ivanov, R. Liseau, M. Meyer, G. Oloffson, I. Pagano, G. Piotto, D. Pollacco, D. Queloz, R. Ragazzoni, E. Renotte, M. Steller, and N. Thomas, "CHEOPS: A transit photometry mission for ESA's small mission programme," in *European Physical Journal Web of Conferences*, *European Physical Journal Web of Conferences* **47**, p. 3005, Apr. 2013.
2. D. Titov, S. Barabash, L. Bruzzone, M. Dougherty, L. Duvet, C. Erd, L. Fletcher, R. Gladstone, O. Grasset, L. Gurvits, P. Hartogh, H. Hussmann, L. Iess, R. Jaumann, Y. Langevin, P. Palumbo, G. Piccioni, and J.-E. Wahlund, "JUICE: The ESA Mission to Study Habitability of the Jovian Icy Moons," *LPI Contributions* **1774**, p. 4035, Feb. 2014.
3. V. Martínez Pillet, "The ESA/NASA mission Solar Orbiter," in *IAC Talks, Astronomy and Astrophysics Seminars from the Instituto de Astrofísica de Canarias*, p. 305, May 2012.
4. R. Laureijs, P. Gondoin, L. Duvet, G. Saavedra Criado, J. Hoar, J. Amiaux, J.-L. Auguères, R. Cole, M. Cropper, A. Ealet, P. Ferruit, I. Escudero Sanz, K. Jahnke, R. Kohley, T. Maciaszek, Y. Mellier, T. Oosterbroek, F. Pasian, M. Sauvage, R. Scaramella, M. Sirianni, and L. Valenziano, "Euclid: ESA's mission to map the geometry of the dark universe," in *Society of Photo-Optical Instrumentation Engineers (SPIE) Conference Series*, *Society of Photo-Optical Instrumentation Engineers (SPIE) Conference Series* **8442**, Sept. 2012.
5. C. Barban, M. J. Goupil, H. Rauer, and Plato 2. 0 Team, "The Space Mission PLATO 2.0, a Medium Class ESA Project," in *Astronomical Society of the Pacific Conference Series*, K. Jain, S. C. Tripathy, F. Hill, J. W. Leibacher, and A. A. Pevtsov, eds., *Astronomical Society of the Pacific Conference Series* **478**, p. 115, Dec. 2013.
6. SPICA Study Team Collaboration, "SPICA Assessment Study Report for ESA Cosmic Vision 2015-2025 Plan," *ArXiv e-prints* , Jan. 2010.
7. *Space Systems-Definition of the Technology Readiness Levels (TRLs) and their criteria of assessment*, no. ISO 16290:2013(E), ISO, 2013.
8. "European space agency cosmic vision 2015-2025 technology development plan programme of work 2009-2014 and related procurement plan."

9. K. D. Irwin, "An application of electrothermal feedback for high resolution cryogenic particle detection," *Applied Physics Letters* **66**, pp. 1998–2000, Apr. 1995.
10. P. Roelfsema, M. Giard, F. Najarro, K. Wafelbakker, W. Jellema, B. Jackson, B. Swinyard, M. Audard, Y. Doi, M. Griffin, F. Helmich, F. Kerschbaum, M. Meyer, D. Naylor, H. Nielsen, G. Olofsson, A. Poglitsch, L. Spinoglio, B. Vandenbussche, K. Isaak, and J. R. Goicoechea, "The SAFARI imaging spectrometer for the SPICA space observatory," in *Society of Photo-Optical Instrumentation Engineers (SPIE) Conference Series*, *Society of Photo-Optical Instrumentation Engineers (SPIE) Conference Series* **8442**, Sept. 2012.
11. T. Nakagawa, H. Matsuhara, and Y. Kawakatsu, "The next-generation infrared space telescope SPICA," in *Society of Photo-Optical Instrumentation Engineers (SPIE) Conference Series*, *Society of Photo-Optical Instrumentation Engineers (SPIE) Conference Series* **8442**, Sept. 2012.
12. D. J. Goldie, J. R. Gao, D. M. Glowacka, D. K. Griffin, R. Hijmering, P. Khosropanah, B. D. Jackson, P. D. Mauskopf, D. Morozov, J. A. Murphy, M. Ridder, N. Trappe, C. O'Sullivan, and S. Withington, "Ultra-low-noise transition edge sensors for the SAFARI L-band on SPICA," in *Society of Photo-Optical Instrumentation Engineers (SPIE) Conference Series*, *Society of Photo-Optical Instrumentation Engineers (SPIE) Conference Series* **8452**, Sept. 2012.
13. P. Khosropanah, R. Hijmering, M. Ridder, J. R. Gao, D. Morozov, P. D. Mauskopf, N. Trappe, C. O'Sullivan, A. Murphy, D. Griffin, D. Goldie, D. Glowacka, S. Withington, B. D. Jackson, M. D. Audley, and G. de Lange, "TES arrays for the short wavelength band of the SAFARI instrument on SPICA," in *Society of Photo-Optical Instrumentation Engineers (SPIE) Conference Series*, *Society of Photo-Optical Instrumentation Engineers (SPIE) Conference Series* **8452**, Sept. 2012.
14. R. H. den Hartog, M. P. Bruijn, A. Clenet, L. Gottardi, R. Hijmering, B. D. Jackson, J. van der Kuur, B. J. van Leeuwen, A. J. van der Linden, D. van Loon, A. Nieuwenhuizen, M. Ridder, and P. van Winden, "Progress on the FDM Development at SRON: Toward 160 Pixels," *Journal of Low Temperature Physics* , Feb. 2014.
15. L. Puig, K. G. Isaak, M. Linder, I. Escudero, D. Martin, P.-E. Crouzet, L. Gaspar Venancio, and A. Zuccaro Marchi, "Status of the assessment phase of the ESA M3 mission candidate EChO," in *Society of Photo-Optical Instrumentation Engineers (SPIE) Conference Series*, *Society of Photo-Optical Instrumentation Engineers (SPIE) Conference Series* **8442**, Sept. 2012.
16. C. W. McMurtry, D. Lee, J. Beletic, C. Chen, R. Demers, M. Dorn, D. Edwall, C. Bacon Fazar, W. J. Forrest, F. Liu, A. K. Mainzer, J. Pipher, and A. Yulius, "Development of Passively Cooled Long Wave Infrared Detector Arrays for NEOCam," in *American Astronomical Society Meeting Abstracts*, *American Astronomical Society Meeting Abstracts* **221**, p. 350.04, Jan. 2013.
17. "Echo assessment study report," Tech. Rep. ESA/SRE(2013)2, ESA, 2013.
18. "Characterisation activities of new nir to vlwir detectors from selex es ltd at the ukatc," (Paper 9154-12 this conference), 2014.
19. D. Atkinson, N. Bezawada, L. G. Hipwood, N. Shorrocks, and H. Milne, "Operation and performance of new NIR detectors from SELEX," in *Proc. SPIE , High Energy, Optical, and Infrared Detectors for Astronomy V*, **8453**, 2012.
20. O. Gravrand, L. Mollard, O. Boulade, V. Moreau, E. Sanson, and G. Destéfanis, "Ultra low dark current CdHgTe FPAs in the SWIR range at CEA and Sofradir," in *Society of Photo-Optical Instrumentation Engineers (SPIE) Conference Series*, *Society of Photo-Optical Instrumentation Engineers (SPIE) Conference Series* **8176**, Oct. 2011.
21. D. Golimowski, J. Anderson, A. Armstrong, S. Arslanian, L. Bedin, R. Bohlin, K. Boyce, G. Chapman, E. Cheng, M. Chiaberge, C. Cox, T. Desiardins, D. Dye, T. Ellis, B. Ferguson, A. Fruchter, N. Grogin, P. L. Lim, M. Loose, R. Lucas, O. Lupie, J. Mack, A. Maybhate, K. Mil, M. Mutchler, R. Ricardo, B. Scott, B. Serrano, M. Sirianni, L. Smith, A. A. Suchkov, A. Waczynski, A. Welty, T. Wheeler, and E. Wilson, "ACS after SM4: New Life for an Old Workhorse," in *Hubble after SM4. Preparing JWST*, July 2010.
22. *Space engineering: Spacewire-links, nodes, routers and networks*, no. ECSS-E-ST-50-12C, ECSS European Coorperation for Space Standardization, 2008.
23. "Microelectronics technogies for space."
24. "Development of an asic for the readout and control of near-infrared large array detectors," (Paper 9154-71, this conference), 2014.

25. J. Endicott, A. Walker, S. Bowring, P. Turner, D. Allen, O. Piersanti, A. Short, and D. Walton, "Charge-coupled devices for the ESA PLATO M-class Mission," in *Society of Photo-Optical Instrumentation Engineers (SPIE) Conference Series*, *Society of Photo-Optical Instrumentation Engineers (SPIE) Conference Series* **8453**, July 2012.
26. *Photosensitive Charge coupled devices and CMOS imaging sensors with Hermetic and non-hermetic packages*, no. 2, ESCC Europena Space Component Specifications, March 2010.
27. J. P. D. Gow, N. J. Murray, A. D. Holland, D. J. Hall, M. Cropper, D. Burt, G. Hopkinson, and L. Duvet, "Assessment of space proton radiation-induced charge transfer inefficiency in the CCD204 for the Euclid space observatory," *Journal of Instrumentation* **7**, p. C1030, Jan. 2012.
28. J. Gow, N. J. Murray, A. D. Holland, D. Burt, and P. Pool, "A comparative study of proton radiation damage in p- and n-channel CCDs," in *Society of Photo-Optical Instrumentation Engineers (SPIE) Conference Series*, *Society of Photo-Optical Instrumentation Engineers (SPIE) Conference Series* **7435**, Aug. 2009.
29. D. H. Lumb, "CCD radiation damage in ESA Cosmic Visions missions: assessment and mitigation," in *Society of Photo-Optical Instrumentation Engineers (SPIE) Conference Series*, *Society of Photo-Optical Instrumentation Engineers (SPIE) Conference Series* **7439**, Aug. 2009.
30. J. P. D. Gow, N. J. Murray, A. D. Holland, D. Burt, and P. J. Pool, "Comparison of proton irradiated P-channel and N-channel CCDs," *Nuclear Instruments and Methods in Physics Research A* **686**, pp. 15–19, Sept. 2012.
31. "Assessment of the performance and radiation damage effects under cryogenic temperatures of a p-channel ccd204," (Paper 9154-99, this conference), 2014.
32. F. G. A. Quarati, M. S. Alekhin, K. W. Krämer, and P. Dorenbos, "Co-doping of $CeBr_3$ scintillator detectors for energy resolution enhancement," *Nuclear Instruments and Methods in Physics Research A* **735**, pp. 655–658, Jan. 2014.
33. L. Amati, J.-L. Atteia, L. Balazs, S. Basa, J. Becker Tjus, D. F. Bersier, M. Boer, S. Campana, B. Ciardi, S. Covino, F. Daigne, M. Feroci, A. Ferrara, F. Frontera, J. P. U. Fynbo, G. Ghirlanda, G. Ghisellini, S. Glover, J. Greiner, D. Gotz, L. Hanlon, J. Hjorth, R. Hudec, U. Katz, S. Khochfar, R. Klessen, M. Kowalski, A. J. Levan, S. McBreen, A. Mesinger, R. Mochkovitch, P. O'Brien, J. P. Osborne, P. Petitjean, O. Reimer, E. Resconi, S. Rosswog, F. Ryde, R. Salvaterra, S. Savaglio, R. Schneider, G. Tagliaferri, N. R. Tanvir, and A. van der Horst, "Light from the Cosmic Frontier: Gamma-Ray Bursts," *ArXiv e-prints* , June 2013.
34. M. A. J. van Pamelen and C. Budtz-Jørgensen, "Novel electrode geometry to improve performance of CdZnTe detectors," *Nuclear Instruments and Methods in Physics Research A* **403**, pp. 390–398, Feb. 1998.
35. P. Lechner, S. Eckbauer, R. Hartmann, S. Krisch, D. Hauff, R. Richter, H. Soltau, L. Strüder, C. Fiorini, E. Gatti, A. Longoni, and M. Sampietro, "Silicon drift detectors for high resolution room temperature X-ray spectroscopy," *Nuclear Instruments and Methods in Physics Research A* **377**, pp. 346–351, Feb. 1996.
36. C. Fiorini, L. Bombelli, P. Busca, A. Marone, R. Peloso, R. Quaglia, P. Bellutti, M. Boscardin, F. Ficorella, G. Giacomini, A. Picciotto, C. Piemonte, N. Zorzi, N. Nelms, and B. Shortt, "Silicon Drift Detectors for Readout of Scintillators in Gamma-Ray Spectroscopy," *IEEE Transactions on Nuclear Science* **60**, pp. 2923–2933, Aug. 2013.
37. D. Koschny, A. Marino, and J. Oberst, "A camera for observing meteors from space - the Smart Panoramic Camera Head (SPOSH)," in *Proceedings of the International Meteor Conference, 24th IMC, Oostmalle, Belgium, 2005*, L. Bastiaens, J. Verbert, and J.-M. Wislez, eds., pp. 99–104, Aug. 2006.
38. "Ccd characterisation for space missions at esa," (Paper 9154-15, this conference), 2014.
39. P.-E. Crouzet, J. ter Haar, F. de Wit, T. Beaufort, B. Butler, H. Smit, C. van der Luijt, and D. Martin, "Test set up description and performances for HAWAII-2RG detector characterization at ESTEC," in *Society of Photo-Optical Instrumentation Engineers (SPIE) Conference Series*, *Society of Photo-Optical Instrumentation Engineers (SPIE) Conference Series* **8453**, July 2012.
40. P. Verhoeve, N. Boudin, U. Telljohann, T. Oosterbroek, D. Martin, L. Duvet, T. Beaufort, B. Butler, I. Escudero-Sanz, H. Smit, and F. de Wit, "ESA's CCD test bench for the Euclid visible channel," in *Society of Photo-Optical Instrumentation Engineers (SPIE) Conference Series*, *Society of Photo-Optical Instrumentation Engineers (SPIE) Conference Series* **8453**, July 2012.

41. N. Boudin, P. Verhoeve, H. Smit, U. Telljohann, L. Duvet, and D. Martin, "Preliminary results of CCD characterisation at ESA in support of the Euclid visible channel," in *Society of Photo-Optical Instrumentation Engineers (SPIE) Conference Series*, *Society of Photo-Optical Instrumentation Engineers (SPIE) Conference Series* **8453**, July 2012.
42. "A comparative study of charge transfer inefficiency value and trap parameter determination techniques making use of an irradiated esa-euclid prototype ccd," (Paper 9154-33 this conference), 2014.
43. "Laboratory simulation of euclid-like sky images to study the impact of ccd radiation damage on weak gravitational lensing," (Paper 9154-52, this conference), 2014.
44. P.-E. Crouzet, J. ter Haar, F. de Wit, T. Beaufort, B. Butler, H. Smit, C. van der Luijt, and D. Martin, "Characterization of HAWAII-2RG detector and SIDECAR ASIC for the Euclid mission at ESA," in *Society of Photo-Optical Instrumentation Engineers (SPIE) Conference Series*, *Society of Photo-Optical Instrumentation Engineers (SPIE) Conference Series* **8453**, July 2012.
45. Y.-R. Nowicki-Bringuier and P. Chorier, "Sofradir SWIR hyperspectral detectors for space applications," in *Society of Photo-Optical Instrumentation Engineers (SPIE) Conference Series*, *Society of Photo-Optical Instrumentation Engineers (SPIE) Conference Series* **7474**, Sept. 2009.